Lançadores Espaciais[☆] (1st year, MEAer)

Academic Year 2024/25

Group 1, 12-P Combination of air-breathing and rocket engines

Paulo J. S. Gil[a,*], João Teixeira Borges[b], Rafael Azeiteiro ist1102478, Eduardo Helena ist1102793, Elena Francesca Cipriano ist112514, Denis Ring ist112102, Guilherme Martins ist1112118, Érica Vita ist1112267, Gonçalo Coelho ist1112327

[a] *ACMAA, Instituto Superior Técnico, Universidade de Lisboa*
[b] *ACTTCE, Instituto Superior Técnico, Universidade de Lisboa*

Abstract

This report presents a concise theoretical and numerical analysis of ramjet propulsion for hypersonic flight, evaluating engine performance through both ideal and real-cycle models under varying operational conditions. It also compares traditional ramjets with alternative propulsion systems, such as pre-cooled air-breathing rocket engines, to provide insights into optimizing efficiency and feasibility for advanced aerospace applications. It was concluded that various parameters—such as free-stream temperature, inlet Mach number, burner temperature, burner Mach number, and shock strength—significantly influence the overall efficiency of a ramjet engine.

Keywords: Hypersonic flight, air-breathing propulsion, ramjet engines, numerical modeling, high-Mach propulsion, pre-cooled engines, software analysis.

Contents

[☆] Space Launchers.
[*] In charge of course.

Email addresses: paulo.gil@tecnico.ulisboa.pt (Paulo J. S. Gil), tborges@hidro1.ist.utl.pt (João Teixeira Borges)

1. Introduction

1.1. Motivation and Objectives

It is often said, yet remains a fundamental truth, that since the dawn of aviation, humanity has continuously pushed the boundaries of flight—striving not only to reach higher altitudes but also to achieve, interestingly enough, ever-increasing speeds.

With this in mind, this project begins by analyzing the topic of hypersonic flight, with a specific focus on air-breathing propulsion. The primary objective is to explore the available options and challenges associated with this field.

Specifically, the study will focus on Ramjet Engines, transitioning from a theoretical characterization of their operation to the development of a Simplified Design Numerical Software to support their thermodynamics analysis and design.

John Drury Clark stated in *Ignition!: An Informal History of Liquid Rocket Propellants*, "The engineers had been guilty of a sin to which engineers are prone—starting their engineering before doing their research." [1]. Let us challenge this notion, demonstrating that in this project rigorous engineering and research go hand in hand.

1.2. Project Layout

This project is structured into six main chapters.

Chapter 1 introduces the project's motivation and goals, along with a roadmap of the document. Following, chapter 2 provides background on High Mach/Hypersonic Air-Breathing Propulsion, emphasizing its benefits and relevance. Chapter 3 focuses on the Ramjet Engine as a selected solution, detailing its types and underlying thermodynamic principles, on the other hand, chapter 4 examines alternative engine concepts, comparing their main features and performance metrics. Chapter 5 shifts to the second project objective: developing a software tool for Ramjet Engine numerical analysis and preliminary design. Finally, chapter 6 concludes the project, and Appendix A includes the required Group Intra-Evaluation for the course.

2. High Mach/Hypersonic Air Breathing Propulsion

By definition, supersonic flight occurs when an aircraft or object moves through the air at speeds exceeding the local speed of sound. When speeds surpass approximately five times the speed of sound (Mach 4-5), the term hypersonic flight is employed [2].

Historically, rocket boosters have been used to propel hypersonic vehicles however, air-breathing high-Mach and hypersonic propulsion offer significant advantages for sustained atmospheric flight and orbital insertion [3]. Unlike rockets, which must carry onboard oxidizers, these engines utilize atmospheric oxygen, reducing weight and propulsion requirements. By eliminating the need for onboard oxidizers, airbreathing propulsion systems enhance range, payload capacity, and efficiency [4].

A critical challenge in hypersonic flight is the extreme thermal, aerodynamic, and structural loads, which render conventional turbine engines ineffective. Turbojets, for instance, are limited by the maximum rotational speed of the rotor and the permissible turbine inlet

temperature, impacting blade durability and overall engine reliability. These limitations constrain operational flight speeds [4].

Ramjets and scramjets (supersonic combustion ramjets) address this challenge by leveraging high-speed airflow to compress incoming air without the need for rotating components. This "ram" effect enables efficient high-speed propulsion [4]. The design of both ramjet and scramjet engines must ensure sufficient pressure increase within the engine to generate enough thrust to overcome vehicle drag, enabling sustained flight [3]. Successfully achieving this requires addressing several technical challenges, which are illustrated in Figure 2.

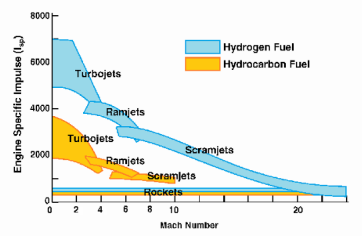

Figure 1: Operation envelopes and efficiency of different engine types [5].

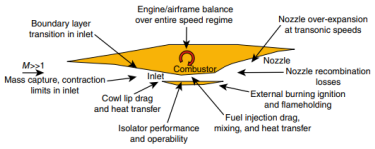

Figure 2: Engine issues for hypersonic airbreathing propulsion systems [3].

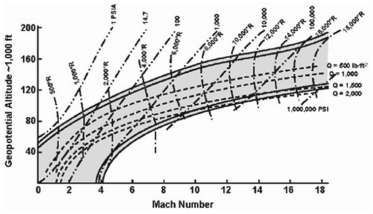

Figure 3: Typical flight corridor for airbreathing engines [6].

Specific impulse (Isp) serves as a key metric for comparing engine efficiencies and performance. Figure 1 illustrates specific impulse versus Mach number for different propulsion systems. Hydrogen-fueled engines demonstrate superior efficiency over hydrocarbon-based systems. Furthermore, at Mach numbers above 6–7, only rockets and scramjets remain viable, with scramjets offering a significant advantage in specific impulse over rockets.

Airbreathing vehicles operate at high dynamic pressure q to ensure sufficient static pressure at the combustor inlet for stable combustion and adequate thrust. To maintain constant dynamic pressure throughout flight, Mach number and altitude must vary accordingly—higher altitudes require increased speed due to lower air density [6].

Figure 3 illustrates a typical Mach-altitude flight corridor for airbreathing engines. The upper boundary is constrained by low ambient pressure and density, leading to reduced combustion efficiency. The lower boundary is defined by material limitations due to increased pressure loads and skin temperatures. At higher Mach numbers, rising total temperatures induce dissociation, structural heating, and combustion inefficiencies, while at lower Mach numbers, insufficient combustor inlet pressure and temperature hinder efficient combustion. Within this corridor, various engine concepts exist to extend operational range, including ejector ramjets, turbo-ramjets, turbo-ramjet rockets, precooled air-breathing engines, liquid air cycle engines, and inverse cycle engines.

3. Ramjet Engine

3.1. Fundamentals

The ramjet is an air-breathing engine that utilizes the vehicle's speed to compress and decelerate incoming air through the ram effect in a fixed duct. Its key components are

illustrated in Figure 4. Air enters the intake, where it is compressed by the spike and slowed to subsonic speeds at the combustor inlet. Inside the combustor, fuel mixes with air and burns, stabilized by a flame holder. The resulting exhaust expands through the nozzle at a velocity higher than the intake flow, producing forward thrust.

A pure ramjet engine relies solely on air compression from velocity reduction in the inlet, achieved through a complex shock structure. As it lacks static thrust capability, an auxiliary engine, typically rocket boosters, is required to provide the initial "Mach kick".

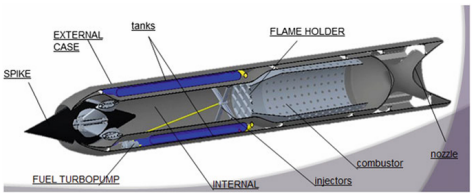

Figure 4: Elements of a Ramjet Engine [6].

3.2. Ideal Ramjet Cycle

The ideal ramjet cycle consists of three main processes: isentropic compression through the inlet, isobaric heat addition in the combustor, and isentropic expansion through the nozzle, seen in Figure 5a. It operates without any moving parts, relying entirely on high-speed forward motion to compress incoming air. The thermal and propulsive efficiencies are determined by the Mach number and temperature ratios across the cycle.

The ideal ramjet cycle is a variation of the Brayton cycle adapted for high-speed air-breathing propulsion, where the compressor and turbine stages are replaced by aerodynamic compression and direct exhaust expansion. Incoming air enters the engine at a flight Mach number M_0 and is subsequently decelerated to subsonic speeds through a convergent-divergent diffuser.

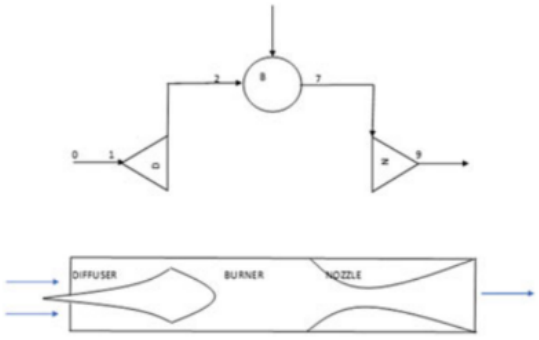

(a) Sketch of the ideal ramjet cycle. Taken from [6].

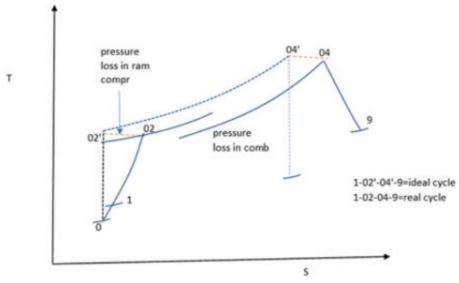

(b) T-S diagram of the Brayton cycle. Taken from [6].

Figure 5: Ideal ramjet cycle and corresponding Brayton T-S diagram.

Analyzing the ideal ramjet Brayton cycle, it is possible to identify the key thermodynamic stations, mentioned earlier, along the flow path. Assuming isentropic compression at the inlet, the total pressure and total temperature remain unchanged between the free stream and the inlet, designated as stations 0 to 02' in Figure 5b.

The addition of heat due to the combustion process occurs at constant pressure and is represented by the isobaric line between stations 02' and 04' in Figure 5b, during which the total temperature increases significantly.

Finally, the expansion process through the nozzle is idealized as an isentropic expansion and is represented by station 9. This expansion converts thermal energy into kinetic energy, producing thrust.

It is important to note that the ideal ramjet cycle neglects real-world losses such as shock-induced pressure drops, friction, heat transfer to the walls, and non-ideal mixing and combustion. These effects - mentioned in the next chapter - reduce the actual efficiency and performance compared to the idealized model.

3.3. Real Ramjet Cycle

For the real thermodynamic cycle of a ramjet, assuming no frictional losses, uniform temperature and velocity in the direction of the flow, and considering a decrease in stagnation pressure during the combustion process, the momentum equation can be applied to analyze the flow dynamics and quantify the effects of these conditions on the overall performance of the engine. The following equation represents the momentum equation:

$$(p_3 - p_4) \times A - D = \dot{m}_4 \times u_4 - \dot{m}_3 \times u_3 \tag{1}$$

where D represents the flow drag induced by the flame holders. The primary reason for the discrepancy between the real and theoretical cycles is that this drag is dependent on a correction factor K. Consequently, the drag force D can be expressed as [6]:

$$D = K \left(\frac{1}{2} \times \rho_3 \times u_3^2 \right) \tag{2}$$

Note that, Station 3 represents combustor inlet conditions without Rayleigh effects, while Station 4 corresponds to the combustor exit. The equation illustrates that when K = 0, which indicates that there are no losses, the combustion process follows the behavior of the Rayleigh flow. For K=1, losses are attributed solely to the presence of the flame holder, while for K=2, both flame-holder-induced losses and frictional losses are accounted for in the analysis [6].

According to Fanno Flow and Rayleigh flow theory, the Mach number increases toward the limit value (when thermal choking takes place) $M_4 = 1$ [6]. Therefore, for a real flow there's a drag component in the mix of things, which will increase the pressure losses of the system.

3.4. Ramjet Thrust and Performance Considerations

The theoretical thrust concept for a ramjet follows the same fundamental principles as any other propulsion system. However, in addition to specific impulse, the ramjet is often characterized by its specific thrust, which is defined as the thrust produced per unit mass flow rate of air:

$$S = \frac{F}{\dot{m}_a} \quad \left[\frac{\mathrm{N}}{\mathrm{kg/s}}\right] \tag{3}$$

where:

- S is the specific thrust [$\mathrm{N \cdot s/kg}$]; F is the net thrust [N]; $\dot{m}_a$ is the air mass flow rate

This equation highlights several key aspects of ramjet operation:

- **Lack of Static Thrust:** As a result, they typically require an auxiliary propulsion system, such as a rocket booster, for takeoff and acceleration to operational speeds.

- **Dependence on Ram Compression:** The ramjet relies solely on aerodynamic compression of incoming air, eliminating the need for mechanical compressors or turbines. Consequently, it requires high flight speeds to achieve efficient compression and sufficient pressure recovery at the inlet.

- **Burner Stagnation Temperature Increase:** The overall performance of the engine is strongly influenced by the rise in stagnation temperature across the burner, which directly impacts the available energy for expansion through the nozzle and thus the thrust generation.

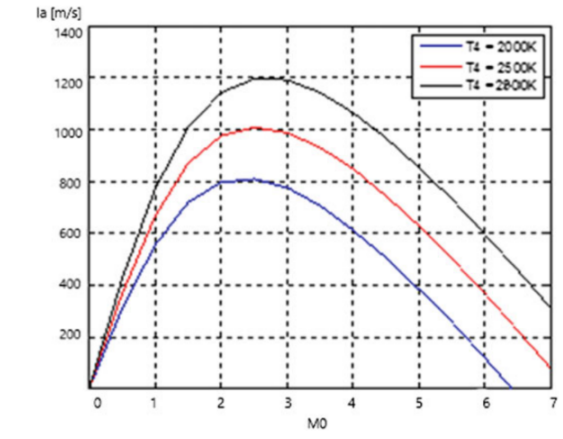

Figure 6: S versus M_0 for a stoichiometric combustion. Taken from [6].

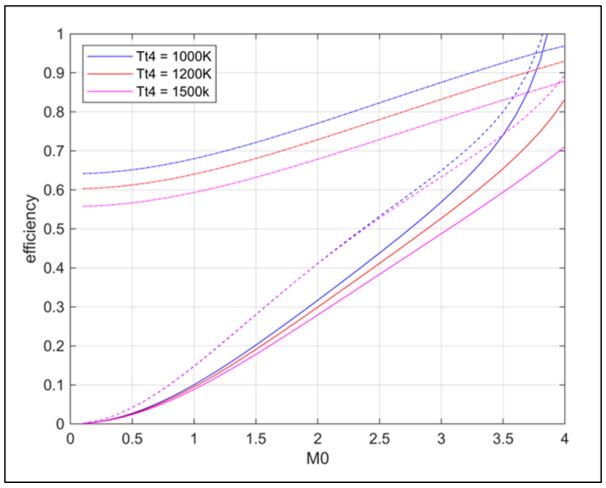

Figure 7: Efficiency variation with Mach number: thermal (dashed), propulsive (dash-dot), and overall efficiency (solid). Taken from [7].

Figure 6 shows the variation of specific thrust S as a function of flight Mach number M_0 for three different burner exit temperatures (T_4 = 2000 K, 2500 K, and 2800 K), at a stoichiometric equivalence ratio ($\Phi = 1$). The curves demonstrate several important trends in ramjet performance.

At low Mach numbers, specific thrust increases sharply with increasing M_0. This is due to greater kinetic energy of the incoming flow being converted into pressure and thermal energy in the burner, enabling more expansion and thus higher thrust.

Each curve reaches a peak value of S at a certain optimal Mach number (around $M_0 =$ 2.5–3.5 depending on T_4), beyond which specific thrust begins to decline. This decrease is attributed to the rising inlet stagnation temperature at higher Mach numbers, which reduces the effective temperature rise across the combustor and limits the amount of usable thermal energy for thrust generation.

As for T_4, higher burner exit temperatures result in higher peak specific thrust and shift the peak to slightly higher Mach numbers. This is expected, as more thermal energy is available to accelerate the flow in the nozzle. However, practical constraints such as material limits, thermal loading, and chemical dissociation limit the maximum achievable T_4.

Figure 7 illustrates more efficiency characteristics of a ramjet engine in relation to Mach number M_0 for various combustor exit temperatures, specifically the combustion chamber (Tt4 = 1000K, 1200K, and 1500K). It illustrates three key efficiency metrics: thermal efficiency (dashed lines), propulsive efficiency (dash-dot lines), and overall efficiency (solid lines). As expected, and observed on the graph, thermal efficiency increases with Mach number, as higher speeds result in improved air compression and combustion effectiveness.

Propulsive efficiency, however, initially decreases at low Mach numbers due to inefficient exhaust velocity matching but improves at higher speeds as the engine operates more efficiently.

The overall efficiency, being the product of thermal and propulsive efficiency, follows an increasing trend with Mach number, though it decreases as Tt4 increases.

3.5. Flame Stability

Flame stability in ramjet combustors is primarily maintained through the use of flame holders, which promote continuous combustion by creating a recirculation region downstream of the holder. In this region, the cold, often partially premixed, turbulent flow of air and fuel comes into contact with the hot combustion products. The resulting turbulent mixing facilitates heat transfer, allowing the fresh mixture to reach ignition temperature.

However, flame blowout can occur if the velocity of the incoming mixture exceeds the local flame speed, or if the mixture temperature is too low. In such cases, insufficient heat is transferred to initiate or sustain combustion.

The geometry of the flame holder plays a critical role in both flame stability and blowout resistance. In general, increasing the perimeter of the flame holder enhances the blowout velocity, provided the transverse dimensions remain above a certain critical limit. For this reason, complex flame holder geometries—such as radial or concentric gutters and arrays of rods—tend to perform better than simpler conical designs under comparable cross-sectional flow areas. While increasing the cross-sectional area of the rods can further raise the blowout velocity, it also increases flow blockage, which may negatively impact overall combustion efficiency.

Stability limits have been correlated with the step height (or flame holder width) using the Damköhler number under premixed conditions at blowout [6]. The Damköhler number

is defined as the ratio of the flow residence time to the characteristic chemical reaction time. A high Damköhler number indicates that chemical reactions are fast relative to convective cooling, promoting stable combustion. In contrast, a low Damköhler number implies a higher risk of flame blowout due to insufficient reaction rates [6].

3.6. Supersonic vs Subsonic Combustion

Conventional ramjet engines are incapable of generating static thrust, as they rely on ram compression—requiring a certain forward flight velocity—to initiate and sustain thrust production. These air breathing engines, paradoxically cease to produce thrust when subjected to excessively high levels of ram compression. At elevated flight speeds, two factors associated with ram compression adversely impact thrust generation [8]. These factors, are as follows:

1. The inlet total pressure recovery that exponentially deteriorates with flight Mach number;
2. The rising gas temperature in the inlet that cuts back (ΔT_t) burner to eventually zero.

The primary challenge in total pressure recovery for supersonic and hypersonic inlets is the normal shock, which also contributes to the rise in gas temperatures within the burner. Eliminating the normal shock in the inlet would theoretically result in a highly efficient ramjet. However, without a terminal normal shock, the airflow within the inlet would remain supersonic, presenting a significant challenge for fuel combustion. Combustion in a supersonic airstream is inherently inefficient [8]. Despite these difficulties, supersonic combustion ramjets, or scramjets, have been developed out of necessity. These engines offer the potential for the highest fuel-specific impulse among airbreathing propulsion systems at flight speeds exceeding Mach 6 and extending into the suborbital range. However, the upper operational limit of scramjets remains uncertain.

3.7. Fuel

3.7.1. Properties

In recent years, various fuels have been tested for ramjet applications. The first to be studied was JP-4, a blend of kerosene and gasoline, characterized by a low flashpoint (23°C) and relatively high volatility. The latest fuel from the JP series used for these applications is JP-10.

More recently, however, high-density fuels have been considered as alternatives for ramjet propulsion, particularly the RJ fuel family. As shown in Tables 8, RJ fuels exhibit high density, elevated fuel-to-air stoichiometric ratios, lower hydrogen-to-carbon (H/C) ratios, and consequently, reduced reaction heat.

3.7.2. Performance Comparison

Considering an ideal ramjet engine operating at an altitude of 15,000 m, with freestream temperature of $T_0 = 216.65K$ and maximum cycle temperature of $T_4 = 2500K$, the specific thrust and fuel consumption for various fuels are presented as functions of Mach number in Figures 9a and 9b.

Fuel	Density (g/cm$^{3)}$	Heating value (MJ/kg)
JP-4	0.76	43,500
JP-5	0.81	43,025
JP-7	0.79	43,890
JP-8	0.81	43,140
JP-10	0.94	42,106
RJ-4	0.93	42,300
RJ-5	1.08	41,300
RJ-6	1.02	41,500

(a) Density and reaction heat of some fuels

Fuel	Ratio	Stoich. ratio
JP-4	2.00	0.067558
JP-5	1.90	0.068290
JP-7	2.07	0.067194
JP-8	1.91	0.068589
JP-10	1.60	0.070762
RJ-4	1.67	0.070300
RJ-5	1.31	0.072638
RJ-6	1.42	0.072171

(b) Ratio H/C and stoichiometric ratio

Figure 8: Fuel Properties Comparison. Taken from [6].

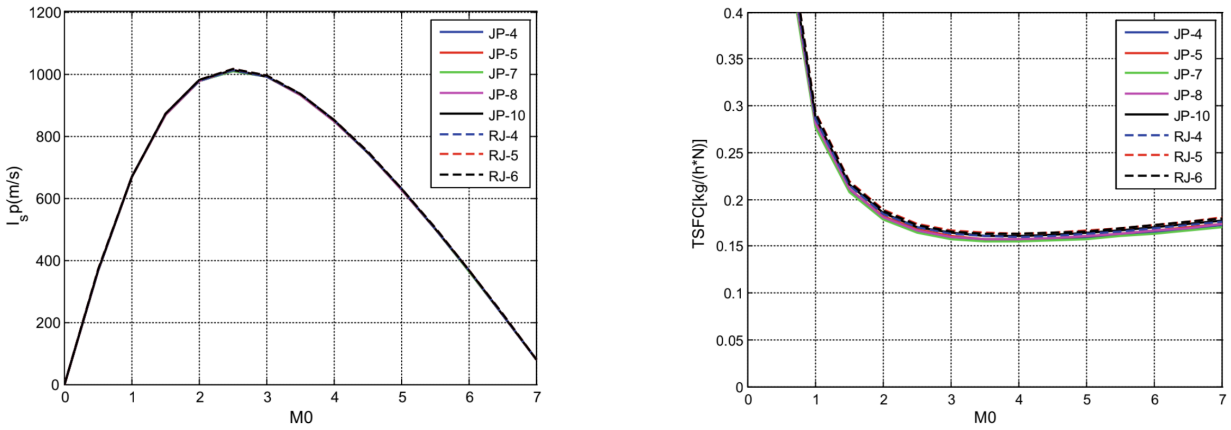

(a) Specific Impulse vs Mach

(b) TSFC vs Mach

Figure 9: Fuel performance comparison as a function of Mach number. Taken from [6].

It can be observed how the differences in performance parameters are practically negligible, so the fuel choice is made based on the fuel's physical properties [6].

JP-4, JP-5, JP-7, and JP-8 exhibit a higher boiling range and volatility compared to fuels like JP-10, which has an almost negligible boiling range, as well as RJ-4 and RJ-5 [6]. Additionally, JP-4, JP-8, and JP-10 have lower freezing points than the RJ family of fuels. JP-4 is particularly flammable, with a flash point of $-23°C$, significantly lower than that of other fuels [6]. Apart from RJ-4, all the mentioned fuels have approximately the same autoignition temperature [6].

The laminar flame speed, presented in Equation 4, refers to the rate at which a flame propagates through a mixture of unburned reactants. This speed is influenced by thermal diffusivity (α), the reaction rate ($\dot{\omega}$), and the temperature distribution within the flame zone [9].

$$s_L^o = \sqrt{\alpha \times \dot{\omega} \times \left(\frac{T_b - T_i}{T_i - T_u}\right)} \tag{4}$$

- u: unburned reactants; b: burned products; i: ignition point

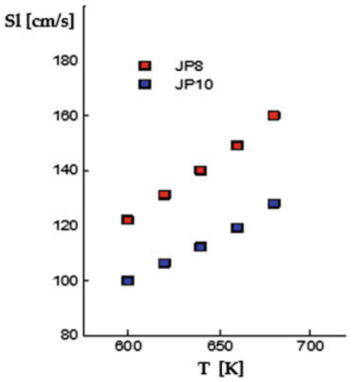

(a) Laminar Flame Speed vs Initial Temperature.

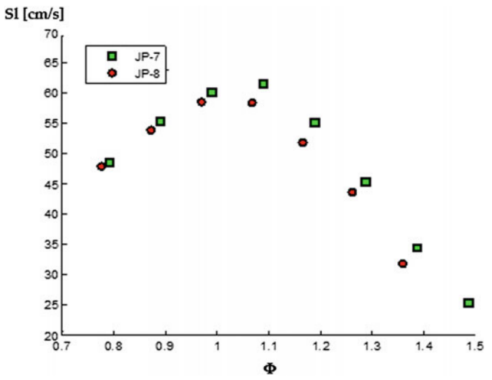

(b) Laminar Flame Speed vs Initial Temperature.

Figure 10: Laminar Flame Speed. Taken from [6].

Both the JP-8 and the JP-10 increase the flame speed with the Initial Temperature (see Figure 10a). For nearly stoichiometric conditions ($\phi = 1$) the JP-7 and JP-8 fuels reach the flame speed's maximum value (see Figure 10b).

- **Applications Requiring Maximizing Specific Thrust:** RJ fuels are recommended. However, their high freezing points make them unsuitable for low-temperature conditions [6].
- **Applications Prioritizing Combustion Efficiency:** JP-7 is the preferred choice due to its stable burning characteristics and higher burning rate compared to other JP fuels [6].
- **Applications Demanding Good Performance at Low Temperatures:** JP-4 is advisable because of its high volatility. However, this also increases the risk of accidental ignition [6].

The choice of fuels depends on the desired application and is a compromise between their chemical and physical properties.

4. Honorable Mention

Before transitioning to the development of the software and modeling aspects of the Ramjet engine, it is valuable to explore other advanced air-breathing propulsion concepts, such as the SABRE and ATREX engines, which integrate innovative technologies to enhance performance across different flight regimes.

4.1. SABRE and ATREX

The Synergetic Air-Breathing Rocket Engine (SABRE) is a hybrid engine developed by Reaction Engines Limited (REL), a British aerospace company. It functions as both a jet

engine for atmospheric flight and a rocket engine for spaceflight, making it a key innovation for reusable spaceplanes like the proposed Skylon spacecraft. [10].

Engineered for single-stage-to-orbit (SSTO) capability, the SABRE engine can accelerate to Mach 5 at an altitude of 25 km in air-breathing mode before transitioning to rocket propulsion. Its inlet operates on a principle similar to that of a ramjet, utilizing the aerodynamic compression known as the "ram effect". Its circulation system uses a heat exchanger to cool incoming air with helium and liquid hydrogen. While the helium cycle increases engine weight, it enhances performance due to helium's high specific heat ratio and reduced cycle pressure ratio [11].

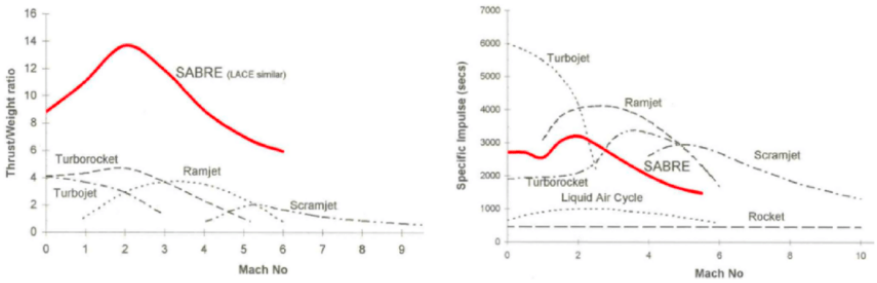

(a) Thrust/weight ratio (b) Specific impulse

Figure 11: Variation with Mach number of thrust–weight ratio and specific impulse of the SABRE. Taken from [12].

As shown in Figure 11, the SABRE engine's thrust-to-weight ratio is significantly higher than other engine types. Additionally, by utilizing atmospheric oxygen for propulsion in the lower atmosphere, it eliminates the need for heavy LOX tanks, reducing overall vehicle weight.

ATREX, a precooled air-breathing engine developed in Japan, demonstrated that precooling negatively impacts specific impulse, particularly at high Mach numbers, due to increased fuel flow reducing efficiency [13].

5. Software Application

A Python-based numerical model was developed to calculate the performance parameters and dimensions required for a ramjet, given initial design operating conditions. The model accepts as inputs free-stream conditions, including flight Mach number, free-stream pressure and temperature, shock strength, burner entry Mach number, burner temperature (combustion chamber limitation), and required thrust.

The core function evaluates key performance outputs such as the inlet area, burner and nozzle areas, as well as thermal, propulsive, and overall cycle efficiencies. It also computes the variation of pressure, temperature, and entropy across four key engine stations: the inlet, post-shock region, burner, and nozzle exit (Fig.12).

The output includes:

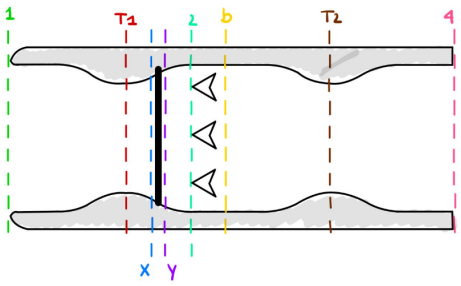

Figure 12: Ramjet Model Representation

- **Geometric parameters:** Inlet Area (A_1), Inlet Throat Area (T_1), Burner Area (b), Nozzle Throat Area (T_2), Exhaust Area (A_4)
- **Efficiency metrics:** Thermal, propulsive, and overall cycle efficiency
- **Thermodynamic profiles:** Temperature and pressure at each engine station
- **Entropy analysis:** Entropy change across the engine cycle for T vs. Δs evaluation

5.1. Theory and Main Assumptions

To successfully develop the software, various assumptions and simplifications were necessary at each stage of the engine. Beginning with the inlet, which will be elaborated in Sec.5.1.1, and extending to the exhaust gases, which are assumed to match the composition and properties of the outside air. Consequently, despite the wide range of temperatures the flow experiences throughout the engine (Fig.13c), normally affecting the Specific Heat Ratio (γ), this value is held constant at 1.4 (γ_{air}) for the entire simulation. This assumption is justified by the findings presented in [14], which demonstrate that, for Mach numbers below 9, as is the case in the present simulation, the variation in γ is negligible. This initial assumption also leads to the specific heat capacities at constant volume (C_v) and pressure (C_p) being treated as constant.

As a result of the assumptions previously described, along with those presented in the subsequent sections, the flow throughout the engine is considered isentropic, except in regions where shock waves occur and within the combustor, where heat addition is modeled. The equations used to describe isentropic flow and shock wave behavior are based on those presented in Chapter 3 of [15].

5.1.1. Assumptions in the Intake

The ramjet intake is designed to slow down supersonic flow and increase pressure before combustion, while minimizing stagnation pressure loss. Typically, it is configured to generate multiple weak oblique shock waves that eventually end in a normal shock wave. In this simulation, for simplicity, the flow compression is modeled using a convergent-divergent geometry, where the supersonic freestream flow is isentropically compressed through the convergent section, throat, and divergent section until the section, downstream of the throat,

where a normal shock wave is positioned, assuming the engine has already completed the starting process. This means that, the shock, initially formed as a standoff shock in front of the intake, moves behind the throat, where it continues compression while minimizing stagnation pressure loss.

To move the shock from its initial position to the one shown in Fig. 12, several methods can be employed: the pilot can increase the craft's speed to move the shock inward (up to Mach 1.8), adjust the area ratio A_1/A_{T1}, or increase the mass flow rate through the engine by "sucking" air through side doors located after the throat. Once inside the nozzle, the shock becomes unstable and will be pushed further until it passes the throat. Regarding the shock itself, it is assumed in the software to have infinitesimal thickness, such that the areas before and after the shock are identical ($A_x = A_y$ in Fig.12).

5.1.2. Assumptions in the Nozzle

In accordance with the ideal Brayton cycle, the flow through the nozzle is simulated as an isentropic expansion, enabling the conditions at station 4 of the engine (Fig.12) to match those of the freestream flow at station 1. This assumption implies a perfectly expanded nozzle with no losses, which, while simplifying the actual process, serves as an approximation for the simulation.

5.1.3. Brayton Cycle and Efficiencies

The combustion process within the ramjet engine model is based on a number of simplifying assumptions, adopted to reduce complexity while retaining physical relevance.

First, the process is assumed to be adiabatic, meaning there is no heat loss to the surroundings. Although in reality some heat transfer does occur—these losses are considered negligible compared to the energy released during combustion and are therefore omitted.

The temperature rise from T_2 to T_b in the combustion chamber is assumed to occur instantaneously. In practice, this transition is governed by the performance of fuel atomizers and flame holders, which control how effectively the fuel and oxidizer mix and burn. Given the high-speed nature of combustion in ramjets, the instantaneous assumption is a reasonable simplification.

The combustion process is also treated as isobaric, with pressure remaining constant throughout the burner. While minor pressure losses do occur due to friction and flow separation, they are neglected here in order to remain consistent with the ideal non-closed Brayton cycle formulation, mentioned in chapter 3.2.

It is further assumed that the combustion is stable, despite the fact that real ramjets may experience pressure oscillations and instabilities. Additionally, the mass of fuel is neglected in the conservation equations. This assumption is justified by the large excess air typically present in ramjet engines, making the fuel mass fraction small enough to be ignored in momentum and energy balances.

The **ideal thermal efficiency**, η_{thermal} for a conventional ramjet cycle [8]:

$$\eta_{\text{ideal thermal}} = 1 - \frac{T_1}{T_2} \tag{5}$$

As for the **real thermal efficiency**, η_{thermal} for a conventional ramjet cycle, is defined as the ratio of the net mechanical energy extracted from the flow to the heat input during combustion, assuming constant specific heat capacity and neglecting fuel mass [8]:

$$\eta_{\text{real thermal}} = \frac{\text{Net Mechanical Output}}{Q_{\text{in}}} = \frac{T_b - T_2 - T_4 + T_1}{T_b - T_2} \tag{6}$$

The **propulsive efficiency**, $\eta_{\text{propulsive}}$, is the ratio of the useful thrust power to the total mechanical energy available in the flow, under the assumptions of one-dimensional steady flow and neglected fuel flow rate [8], this simplifies to:

$$\eta_{\text{propulsive}} = \frac{\text{Thrust Power}}{\text{Net Mechanical Output}} = \frac{2}{1 + \frac{U_4}{U_1}} \tag{7}$$

The overall cycle efficiency is obtained by the product of these two.

5.2. Results

To operate within the hypersonic regime, a flight condition of $M > 5$ is required. As previously discussed, ramjets begin to lose efficiency beyond Mach 5-6, where scramjet technology becomes more favorable. Nevertheless, for advanced high-speed applications such as boost-glide vehicles, hypersonic missiles, or upper-stage propulsion systems, a design point in the Mach 5-6 range remains relevant. Therefore, this operating condition is selected as the reference case to demonstrate the applicability and performance of the developed ramjet model.

To evaluate the ramjet model under hypersonic conditions, a flight scenario was selected at Mach 5 and high altitude, representative of the upper operational boundary for conventional ramjets. The chosen design parameters are:

- Altitude $\approx$ 25–30 km: $P_1 = 2{,}000$ Pa, $T_1 = 220$ K.
- Flight Mach number: $M_1 = 5.0$.
- Shock strength: $M_s = 1.1$ (weak normal shock to reduce stagnation pressure loss).
- Burner entry Mach: $M_2 = 0.3$, following the findings in [8].
- Burner temperature: $T_b = 2600$ K, following the findings in [8] - combustor exit temperature may reach stoichiometric levels.
- Required thrust: $F = 15$ kN.

This configuration represents a hypersonic cruise case at the upper end of ramjet applicabilit. At these speeds, the ram effect is highly effective, allowing for sufficient compression without moving parts. However, care must be taken to manage stagnation pressure losses, thermal loading, and material limitations.

Table 1: Ramjet Design Results at Hypersonic Cruise Conditions ($M_1 = 5.0$)

Parameter	**Value**
Inlet Area (A_1)	0.6167 m^2
Inlet Throat Area (A_{T1})	0.0247 m^2
Burner Area (A_2)	0.0503 m^2
Nozzle Throat Area (A_{T2})	0.0317 m^2
Exhaust Area (A_4)	0.8177 m^2
Ideal Thermal Efficiency ($\eta_{\text{ideal-thermal}}$)	84.89%
Real Thermal Efficiency ($\eta_{\text{real-thermal}}$)	80.66%
Propulsive Efficiency ($\eta_{\text{propulsive}}$)	82.38%
Total Efficiency ($\eta_{\text{total}} = \eta_{\text{propulsive}} * \eta_{\text{real-thermal}}$)	66.45%

Table 1 summarizes the preliminary design results (software output). The geometric parameters define the required engine cross-sectional areas, while the efficiencies reflect the performance potential of the engine under previous assumptions.

Figure 13a shows the pressure distribution across the engine stages. As expected, the pressure increases sharply after the inlet due to aerodynamic compression and the presence of a shock. The pressure remains nearly constant across the burner, consistent with the assumption of isobaric combustion. A significant drop is observed at the nozzle exit, where the flow expands to generate thrust. The overall profile validates the thermodynamic assumptions used in the ideal ramjet model.

Figure 13b presents the temperature versus entropy change across the engine. The rise in entropy reflects the irreversibilities associated with the shock (1) and combustion processes (2). The plot also highlights the increase in total temperature through combustion and its subsequent decrease through expansion (3). The entropy increase is particularly pronounced across the shock and burner stages, in line with theoretical expectations.

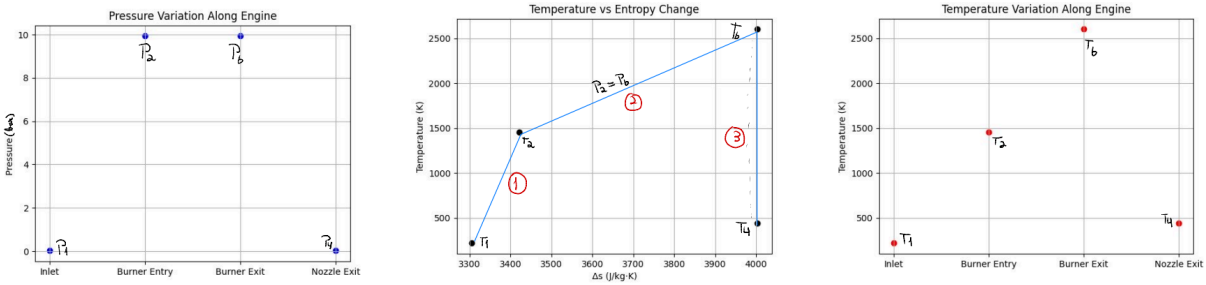

(a) Pressure Variation along the Engine (b) Temperature vs Entropy Change (c) Temperature Variation along the Engine

Figure 13: Overview of relevant parameters along the engine - Software Output

Figure 13c illustrates the temperature variation along the engine. The temperature increases significantly from the inlet to the burner exit, reaching a peak due to combustion. A drop is observed in the nozzle as the high-energy gases expand and accelerate. This temperature profile supports the cycle's energy conversion mechanism—from chemical energy

to kinetic energy—used for thrust production.

5.3. Sensibility Analysis

The variation of thermodynamic and propulsive efficiency is analyzed by varying one parameter at a time from an initial baseline: $P_1 = 70 \times 10^3$, $T_1 = 210$, $M_1 = 2.8$, shock strength = 1.2, $M_2 = 0.2$, $T_b = 1700$, and thrust = 50×10^3. Only cases showing a change in efficiency are presented.

The first case presented in Fig.14a illustrates the variation of the efficiencies as a function of the **freestream Mach number (M_1)**. The results were validated by comparing them with the behavior of a similar engine described in [8] (EXAMPLE 12.13). As shown in both figures, the propulsive efficiency of a ramjet continuously increases with the Mach number, primarily due to the reduction in exit velocity. This decrease in exit velocity is attributed to its relationship with the temperature change (ΔT) from the combustion process ($V_4 = \sqrt{2C_p\Delta T}$); as M_1 increases, greater compression is required in the intake, which leads to higher pre-combustion temperatures and, consequently, a lower ΔT due to the combustion process.

Regarding thermal efficiency, it increases with M_1 until a peak is observed around $M_1 = 5$. This initial increase can be attributed to higher flight speeds, which cause a greater temperature rise in the ramjet's diffuser. As a result, the combustion process becomes more effective at converting fuel energy into useful work, thereby enhancing thermal efficiency. However, beyond a certain Mach number, thermal efficiency plateaus or may even slightly decrease within the engine's operational Mach range. Note that, Fig. 14a extends to higher Mach numbers to illustrate how excessive kinetic energy in the incoming airflow, and consequently, excessively high pre-burning temperatures, lead to inefficiencies in heat addition. To improve the applicable Mach range of the engine, the burner temperature (T_b) should be increased.

With all other parameters fixed, Fig.14b illustrates how the thermal and propulsive efficiencies vary with the **freestream temperature** T_1. Increasing the freestream temperature while keeping the Mach number constant results in a higher cruise velocity (U_1), and consequently, a greater inlet kinetic energy. As indicated by Eq.7 for propulsive efficiency, this leads to an increase in η_{prop} with rising T_1.

On the other hand, regarding thermal efficiency, a higher T_1 while maintaining a constant burner exit temperature (T_b) reduces the thermal potential available for the combustion process. As a result, the heat input becomes less effective in increasing the kinetic energy of the flow, which is reflected in the decreasing trend of η_{thermal}.

As illustrated in Fig. 14c, an increase in the **burner entry Mach number** M_2 leads to a decline in both thermal and propulsive efficiencies. This can be understood by analyzing the parameters influencing these efficiencies: the burner entry temperature T_2 and the outlet velocity U_4. A higher M_2 results in a lower T_2 due to milder compression in the divergent section, leading to a decrease in both ideal and real thermal efficiency. Additionally, the experimentally observed increase in exit velocity U_4 contributes to a reduction in propulsive efficiency.

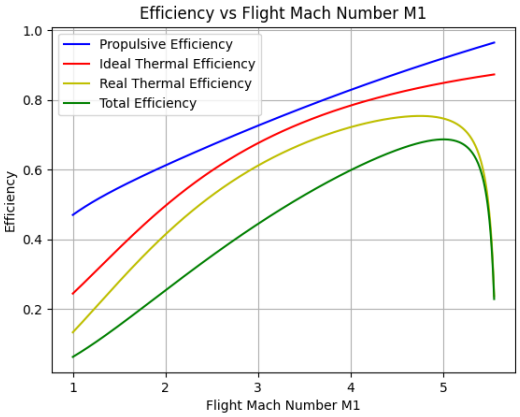

(a) Efficiency vs. Flight Mach Number

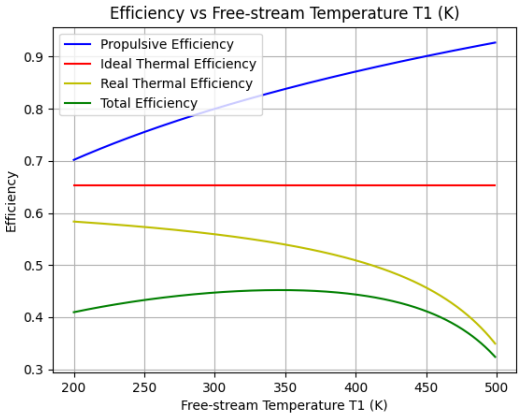

(b) Efficiency vs. Free Stream Temperature

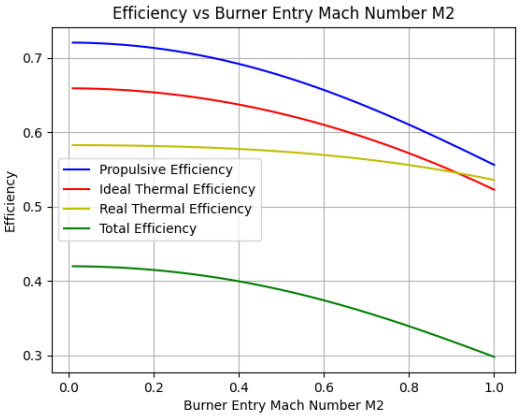

(c) Efficiency vs. Burner Entry Mach Number

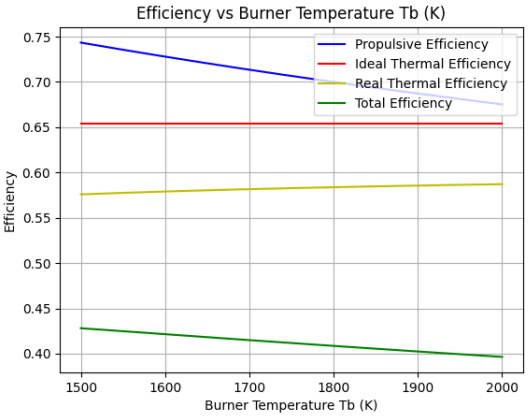

(d) Efficiency vs. Burner Temperature

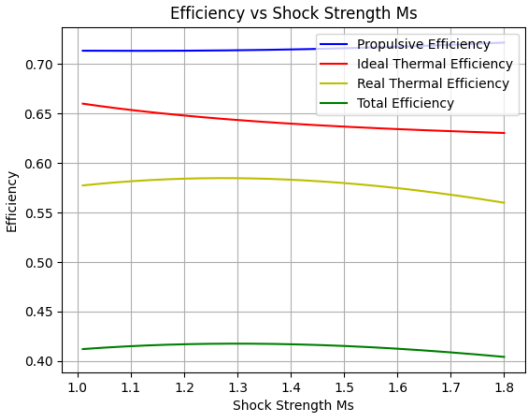

(e) Efficiency vs. Shock Strength

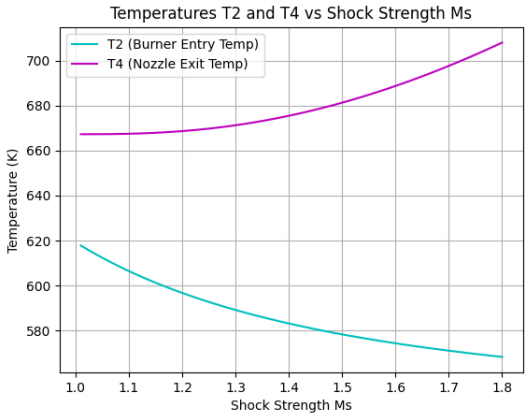

(f) T2 and T4 vs Shock Strength

Figure 14: Ramjet efficiency as a function of flight and design parameters - Software Output

Another parameter considered to provide a comprehensive view of the engine's behavior is the **burner temperature** T_b, which represents the maximum temperature achievable within the combustion chamber. As observable in Fig.14d, increasing the maximum temperature, while ensuring it remains within acceptable structural limits for the combustion chamber, results in a slight improvement in thermal efficiency. This can be attributed to the fact that adjusting this parameter increases the mechanical energy extracted from the flow. However, to achieve this, additional heat must be supplied to the flow, leading to a more mitigated enhancement of the efficiency.

In terms of propulsive efficiency, a hotter burner causes the exhaust gases to exit at much higher speeds, creating a larger mismatch between the jet velocity and the aircraft's speed. As shown in Eq.7, this mismatch results in a lower η_{prop}, as more energy is wasted in the high-speed exhaust rather than being used to generate useful thrust.

Lastly, Fig.14e shows the behavior of $\eta_{\text{propulsive}}$ and η_{thermal} as the **shock strength** M_s increases. While both efficiencies exhibit only small percentage variations overall, indicating that this parameter has a limited effect on engine performance, some noticeable changes still occur. In particular, a stronger shock wave leads to lower stagnation pressure recovery in the intake, reducing the so-called inlet efficiency ($\pi_c = p_{0_2}/p_0$). A lower inlet efficiency (π_r) decreases the pressure available for expansion in the nozzle, ultimately reducing the exhaust velocity (V_e). This, in turn, increases the propulsive efficiency.

Regarding thermal efficiency, the behavior of the real and ideal parameters exhibits only a slight difference. The ideal thermal efficiency, which depends solely on the temperature T_2, decreases as T_2 decreases, as shown in Fig. 14f. In contrast, the real thermal efficiency is influenced not only by the burner entry temperature T_2 but also by the exit static temperature T_4. Specifically, an initial increase in T_4 leads to a slight rise in real thermal efficiency. However, as M_s increases, $\eta_{\text{real,thermal}}$ follows the trend of $\eta_{\text{ideal,thermal}}$, decreasing due to the reduction in T_2.

5.4. Further improvements

Our model assumes that the initial compression is achieved via a converging-diverging diffuser, followed by a normal shock. While this is a common simplification, in reality it results in significant stagnation pressure losses—an undesirable effect in high-speed propulsion.

One method to mitigate these losses is the use of a conical or spiked intake. Such configurations generate oblique shocks upstream of the inlet, reducing flow velocity with smaller entropy increases. The remaining normal shock, now much weaker, causes considerably less total pressure loss.

Ramjets and scramjets often utilize this type of intake design, frequently integrated into the aircraft forebody to take advantage of external and internal oblique shocks. Additionally, the vehicle's angle of attack, α, affects inlet performance by altering shock angles and inlet recovery.

For preliminary analysis, inlet recovery can be assumed based on standard values or referenced from industry standards such as AIA (Aircraft Industries Association) or MIL-E-5008B (Department of Defense) [8]. As shown in Figure 15, the normal shock inlet starts to under perform the other models above Mach 1.6.

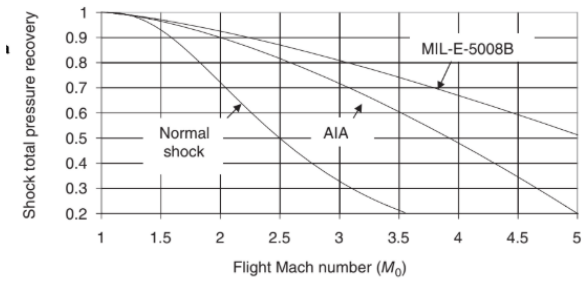

Figure 15: Standards of inlet recovery compared to a normal shock inlet

6. Conclusion

This project provided valuable insights into the theory and design of a ramjet engine.

Among the most important outcomes of the project was a strong understanding of the hypersonic flight regime and its implications for modern aerospace applications. We explored how high Mach number flight influences propulsion system design and operational constraints.

Another major area of learning was the thermodynamic behavior of engines without moving parts. The group investigated how technologies contribute to efficient propulsion without conventional mechanical compression. In parallel, the group gained the ability to critically assess performance metrics, such as thermal and propulsive efficiency, and used them to evaluate the behavior of the engine across a range of flight conditions.

Finally, the development of the numerical solver and plotting tools in Python provided practical experience in software development for propulsion modeling. This process strengthened our skills in algorithm design, numerical analysis, and data visualization

References

[1] J. D. Clark, Ignition!: An Informal History of Liquid Rocket Propellants, Rutgers University Press, New Brunswick, NJ, 1972.

[2] Encyclopædia Britannica, Supersonic flight, accessed: 2025-03-09 (2024).
URL https://www.britannica.com/technology/supersonic-flight

[3] D. M. Van Wie, S. M. D'Alessio, M. E. White, Hypersonic airbreathing propulsion, Johns Hopkins APL Technical Digest 26 (4), accessed: 2025-03-19.

[4] J. F. S. C. d. Magalhães, Design of a single expansion ramp nozzle and numerical investigation of operation at over-expanded conditions, Master's thesis, Universidade da Beira Interior, Covilhã, Portugal, versão corrigida após defesa (2021).

[5] R. Fry, A century of ramjet propulsion technology evolution, Journal of Propulsion and Power 20 (2004) 27–58, accessed: 2025-03-15.

[6] A. Ingenito, Subsonic Combustion Ramjet Design, Springer Briefs in Applied Sciences and Technology, Springer, 2021, accessed: 2025-03-22. doi:10.1007/978-3-030-72809-3.

[7] R. Jakubowski, Aircraft engine construction – ideal ramjet engine, Lecture notes, Rzeszow University of Technology, elaborated by Robert Jakubowski, PhD (n.d.).

[8] S. Farokhi, Aircraft Propulsion, 2nd Edition, John Wiley & Sons, 2014, accessed: 2025-03-22.

[9] L. J. Spadaccini, J. A. TeVelde, Autoignition characteristics of aircraft-type fuels, Tech. Rep. NASA CR-159886, National Aeronautics and Space Administration, Lewis Research Center, Cleveland, Ohio, accessed: 2025-03-22 (June 1980).
URL https://ntrs.nasa.gov/search.jsp?R=19800016175

[10] Wikipedia contributors, SABRE (rocket engine) — Wikipedia, The Free Encyclopedia, accessed: 2025-03-09 (2025).
URL https://en.wikipedia.org/wiki/SABRE_(rocket_engine)

[11] X. Wei, F. Jin, H. Ji, Y. Jin, Thermodynamic analysis of key parameters on the performance of air breathing pre-cooled engine, Applied Thermal Engineering 201 (2021) 117733, accessed: 2025-03-15. doi:10.1016/j.applthermaleng.2021.117733.
URL https://www.researchgate.net/publication/355792204_Thermodynamic_analysis_of_key_parameters_on_the_performance_of_air_breathing_pre-cooled_engine

[12] W. Ma, G. Ma, X. Luo, X. Zhang, J. Liu, F. Liu, Key technologies for thermodynamic cycle of precooled engines: A review, ResearchGateAccessed: 2025-03-10.
URL https://www.researchgate.net/publication/343406065_Key_technologies_for_thermodynamic_cycle_of_precooled_engines_A_review

[13] Z. Qian-nan, The performance optimization of new cycle precooler atrex engine, master's thesis (2017).

[14] K. Xu, F. Liu, C. Cai, One-dimensional multiple-temperature gas-kinetic bhatnagar–gross–krook scheme for shock wave computation, Journal of Computational Physics 203 (1) (2005) 244–261, accessed: 2025-03-22.

[15] J. D. Anderson, Modern Compressible Flow: With Historical Perspective, 3rd Edition, McGraw-Hill Education, New York, 2002, accessed: 2025-03-22.

A. Group Intra-Evaluation

Name	IST Number	Report	Software	Qualitative Evaluation
Guilherme Alexandre Pires Martins	112118	1.1 - Motivation and Objectives 3.3 - Real Ramjet Cycle 3.6 - Supersonic vs Subsonic Combustion	-	14.29
Rafael Coimbra Azeiteiro	102478	2 - High Mach/Hypersonic Air Breathing Propulsion	5.2 - Results 5.3 - Sensibility Analysis	14.29
Érica Vita Amaral Pascoal Cunha	112267	1.2 - Project Layout 3.2 - Ideal Ramjet Cycle 3.4 - Ramjet Thrust and Performance Considerations	-	14.29
Elena Francesca Cipriano	112514	3.4 - Ramjet Thrust and Performance Considerations	5.1 - Theory and Main Assumptions 5.4 - Further improvements	14.29
Gonçalo Pacheco Coelho	112327	3.1 - Fundamentals 3.5 - Flame Stability	-	14.29
Eduardo de Almeida Helena	102793	3.1 - Fundamentals 3.7.1 - Properties 4.1 - SABRE and ATREX	-	14.29
Denis Ring	112102	2 - High Mach/Hypersonic Air Breathing Propulsion 3.7.2 - Performance Comparison 4.1 -SABRE and ATREX	-	14.29

Figure A.16: Group Intra-Evaluation